Rapid Communications

Generalized thermodynamics of phase equilibria in scalar active matter

Alexandre P. Solon,[1] Joakim Stenhammar,[2] Michael E. Cates,[3] Yariv Kafri,[4] and Julien Tailleur[5]
[1]*Massachusetts Institute of Technology, Department of Physics, Cambridge, Massachusetts 02139, USA*
[2]*Division of Physical Chemistry, Lund University, 221 00 Lund, Sweden*
[3]*DAMTP, Centre for Mathematical Sciences, University of Cambridge, Cambridge CB3 0WA, United Kingdom*
[4]*Department of Physics, Technion, Haifa 32000, Israel*
[5]*Université Paris Diderot, Sorbonne Paris Cité, MSC, UMR 7057 CNRS, 75205 Paris, France*

(Received 15 September 2016; revised manuscript received 21 December 2017; published 20 February 2018)

Motility-induced phase separation (MIPS) arises generically in fluids of self-propelled particles when interactions lead to a kinetic slowdown at high densities. Starting from a continuum description of scalar active matter akin to a generalized Cahn-Hilliard equation, we give a general prescription for the mean densities of coexisting phases in flux-free steady states that amounts, at a hydrodynamics scale, to extremizing an effective free energy. We illustrate our approach on two well-known models: self-propelled particles interacting either through a density-dependent propulsion speed or via direct pairwise forces. Our theory accounts quantitatively for their phase diagrams, providing a unified description of MIPS.

DOI: 10.1103/PhysRevE.97.020602

Active materials, composed of particles individually capable of dissipatively converting energy into motion [1–5], display a fascinating range of large-scale properties [6–12]. Among them, motility-induced phase separation [13] (MIPS) has recently attracted a lot of interest [5,13–30]. It arises because self-propelled particles accumulate in regions where they move more slowly [31]. When interactions between particles lead to their slowing down at high density, a positive feedback leads to phase separation between a high-density low-motility phase and a low-density high-motility phase. Remarkably, this liquid-gas phase separation happens without the need of any attractive interactions, leading to the emergence of cohesive matter without cohesive forces. First postulated in idealized toy models [14–20], MIPS has since been addressed experimentally using self-propelled colloids [5,21] and genetically engineered bacteria [32].

The aforementioned instability mechanism leading to MIPS is by now well understood and has been used to define a spinodal region where homogeneous phases are linearly unstable [13,14]. Furthermore, this instability can be understood at the (fluctuating) hydrodynamic level [14,18,25,33,34] where the dynamics of active particles undergoing a kinetic slowdown at high density reduce to an equilibrium model B [35]. On the contrary, there is no comprehensive theory predicting the binodals: the mapping to equilibrium breaks down at higher order in gradients [23] and the corresponding equilibrium predictions for the coexisting binodal densities are violated [23,36].

MIPS has been observed in two broad classes of systems. In a first class of models [14,15,22,33], MIPS arises from an explicit density dependence of the propulsion speed $v(\rho)$. This mimics the way cells adapt their motion to the local density measured through the concentration of a chemical signal, and we refer to such particles as "quorum-sensing active particles" (QSAPs). There, one can define a chemical potential μ [14] which is equal in coexisting phases, but the coexisting pressures, whether mechanical [36] or thermodynamic [23], are unequal. In a second class of models [16–19], particles propelled by a constant force interact via an isotropic, repulsive pair potential; the slowdown triggering MIPS is now due to collisions. Contrary to QSAPs, the mechanical pressure P of such "pairwise-force active particles" (PFAPs), defined as the force density on a confining wall, is equal in coexisting phases. However, an effective chemical potential defined from the thermodynamic equilibrium relation [37] $PV = N\mu - F$ with $\partial F/\partial N = \mu$ takes unequal values in coexisting phases, causing violation of the equilibrium Maxwell equal-area construction [29]. For both models, we thus lack a constraint to complement the equality of pressure (PFAPs) or chemical potential (QSAPs) to fix the values of coexisting densities. The difference between these two classes of models can be shown to stem from whether or not an effective momentum conservation holds in the steady state [38]. When such a conservation law is present, as in PFAPs, the pressure is given by an underlying equation of state and is equal in the two phases [24,29,39]. On the contrary, in the absence of this conservation law, this is generically not the case. All in all, a comprehensive theory of the phase equilibria in MIPS, that would in particular encompass these two different classes of models, remains elusive.

In this Rapid Communication, we propose a unified theory of MIPS based on phenomenological hydrodynamic equations of motion for the scalar density field. We show how the binodals are determined at this level from a common tangent construction on an *effective* free energy density. Our formalism encompasses equilibrium systems for which one recovers the standard thermodynamic free energy and, in that case only, the equality among phases of both pressure and chemical potential. We then show how this generic formalism can be applied to precise models of QSAPs and PFAPs, accounting for their phase diagrams. In particular, we show that different intensive

quantities are equal between coexisting phases in PFAPs and QSAPs.

General framework. We consider a continuum description of active particles with isotropic, nonaligning interactions. In this *scalar* active matter, the sole hydrodynamic field is thus the conserved density $\rho(\mathbf{r},t)$, obeying $\dot{\rho} = -\nabla \cdot \mathbf{J}$. By symmetry, the current $\mathbf{J}$ vanishes in homogeneous phases. Its expansion in gradients of the density involves only odd terms under space reversal. At third order, we use [40]

$$\dot{\rho} = \nabla \cdot (M \nabla g); \quad g = g_0(\rho) + \lambda(\rho)|\nabla\rho|^2 - \kappa(\rho)\Delta\rho. \quad (1)$$

The noiseless hydrodynamic equation (1) describes the evolution of the average coarse-grained density field on scales much larger than the correlation length and time. It can thus be used to characterize fully phase-separated profiles, away from the critical point where noise is irrelevant [41], to predict binodal densities. Equation (1) plays the same role as the Cahn-Hilliard equation does for equilibrium phase-separating systems [41] but in general does not admit an equilibrium free energy structure. In what follows, we first start with Eq. (1) and show how to compute analytically its phase diagram. We then consider a microscopic model of QSAPs for which we obtain the coefficients of Eq. (1) in terms of microscopic parameters by coarse-graining. Finally, we show that our formalism can also be applied to PFAPs, even though closed expressions of the coefficients appearing in (1) are not known explicitly in this case.

Equation (1) predicts a linear instability of a homogeneous profile of density ρ_0 whenever $g_0'(\rho_0) < 0$ [42]: this is the standard linear instability leading to MIPS [14] and defines the spinodal region. We now proceed to establish the corresponding binodals. As in equilibrium, we consider a fully phase-separated system. A macroscopic droplet of the minority phase has an infinite curvature radius, and hence effectively flat interfaces, so that curvature effects are negligible. As in equilibrium, the problem, although n-dimensional, reduces to studying the one-dimensional profile perpendicular to the interface [41]. We thus consider a flat interface, parallel to $\hat{\mathbf{y}}$, between coexisting gas and liquid phases at densities ρ_g and ρ_ℓ. In a steady state with vanishing current, $M\nabla g = 0$, so that g is constant throughout the system: $g(\rho(\mathbf{r},t)) = \bar{g}$. This yields a first equation relating ρ_g and ρ_ℓ:

$$g_0(\rho_g) = g_0(\rho_\ell) = \bar{g}. \quad (2)$$

A second relation can now be obtained by considering a function $R(\rho)$ and integrating $g(\rho)\partial_x R$ across the interface. Replacing $g(\rho)$ by its value $\bar{g}$ or its explicit expression in Eq. (1), one finds two equivalent expressions for $\int_{x_g}^{x_\ell} g(\rho)\partial_x R\, dx$:

$$(R_\ell - R_g)\bar{g} = \phi(R_\ell) - \phi(R_g) + \int_{x_g}^{x_\ell} \left[\lambda(\partial_x\rho)^2 - \kappa\partial_x^2\rho\right]\partial_x R\, dx, \quad (3)$$

where x_g and x_ℓ lie within the bulk gas and liquid phases, $R_{\ell/g} \equiv R(\rho_{\ell/g})$, and ϕ is defined by $d\phi/dR = g_0(\rho)$. To simplify Eq. (3), we choose $R(\rho)$ such that

$$\kappa R'' = -(2\lambda + \kappa')R', \quad (4)$$

where $(')$ denotes $d/d\rho$. Then, one has that

$$\left[\lambda(\partial_x\rho)^2 - \kappa\partial_x^2\rho\right]\partial_x R = -\partial_x\left[\frac{\kappa R'}{2}(\partial_x\rho)^2\right], \quad (5)$$

the integral of which vanishes between any two bulk planes where $\partial_x\rho = 0$. Equation (3) then yields a second constraint:

$$h_0(R_\ell) = h_0(R_g); \quad h_0(R) \equiv R\phi'(R) - \phi(R). \quad (6)$$

Because R is nonlinear in ρ, the lever rule, $\rho_\ell V_\ell + \rho_g V_g = \rho_0 V$ is nonlinear in R, but still determines the phase volumes $V_{\ell,g}$. Also the densities $\rho_{\ell,g}$ do not vary as one moves along the "tie line" by changing the global mean density ρ_0. This is not true generally in nonequilibrium phase separation [43].

Equations (2) and (6) show the coexisting densities to satisfy a common tangent construction on an effective (bulk) free energy $\phi(R) = \int g_0(\rho)dR$. The mathematical similarity with an equilibrium common tangent construction can be traced to the fact that Eq. (1) can be written as

$$\dot{\rho} = \nabla \cdot [M[\rho]\nabla g]; \quad g = \frac{\delta\mathfrak{F}}{\delta R}, \quad (7)$$

with $\mathfrak{F} = \int d\mathbf{r}[\phi(R) + \frac{\kappa}{2R'}(\nabla R)^2]$. The stationary solutions of Eq. (1) then correspond to extrema of the "effective" free energy $\mathfrak{F}$. Note that (7) holds in any dimension. This highlights that, although the construction of the binodals (2)–(6) relies on a single coordinate normal to the interface, our results for the binodals are valid in any dimensions. Last, since $R(\rho)$ is a bijection, the spinodal region is equivalently defined by $d^2\phi/dR^2 < 0$ or $g_0'(\rho) < 0$.

To see how our formalism works, let us first consider an equilibrium case, in which g has an even simpler form

$$g = \frac{\delta\mathcal{F}}{\delta\rho(\mathbf{r})}; \quad \mathcal{F}[\rho] = \int\left[f(\rho) + \frac{c(\rho)}{2}(\nabla\rho)^2\right]d\mathbf{r}. \quad (8)$$

Equation (1) is then the Cahn-Hilliard equation for a system with free energy $\mathcal{F}[\rho]$ and mobility $M[\rho]$ [44]. Equation (8) is consistent with (7) since it imposes $2\lambda + \kappa' = 0$ so that $R = \rho$ (up to an additive and a multiplicative constant which do not affect the phase equilibria) and $\mathfrak{F} = \mathcal{F}$. We recover $\phi(R) = f(\rho)$ as the bulk free energy density, $g_0(\rho) = f'(\rho)$ as the chemical potential, and $h_0(\rho) = f'(\rho)\rho - f(\rho)$ as the pressure.

Our common tangent construction on $\phi(R)$, which amounts to extremizing $\mathfrak{F}$, thus reverts to the usual one in equilibrium, but extends beyond this. We now show how our formalism can be used to derive the phase diagrams of QSAPs and PFAPs.

QSAPs. We consider particles $i = 1 \cdots N$, moving at speeds v_i along body-fixed directions $\mathbf{u}_i$, which undergo both continuous rotational diffusion with diffusivity D_r and complete randomization with tumbling rate α. Each particle adapts its speed $v(\tilde{\rho}_i)$ to the local density

$$\tilde{\rho}_i(\mathbf{r}) = \int d\mathbf{r}' K(\mathbf{r} - \mathbf{r}')\hat{\rho}(\mathbf{r}')d\mathbf{r}' \quad (9)$$

with $K(\mathbf{r})$ an isotropic coarse-graining kernel, and $\hat{\rho}(\mathbf{r}) = \sum_i \delta(\mathbf{r} - \mathbf{r}_i)$ the microscopic particle density.

Deriving hydrodynamic equations from microscopics is generally difficult, even in equilibrium [45]. For QSAPs we

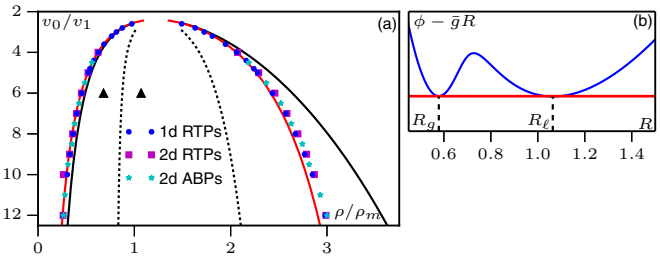

FIG. 1. (a) Phase diagrams of QSAPs. The solid lines correspond to common tangent constructions on $\phi(R)$ (red) or $f(\rho)$ (black). Dashed lines correspond to the spinodals $d^2\phi/dR^2 = 0$. Data points are from simulations of run-and-tumble particles (RTPs; $\alpha = 1$, $D_r = 0$) or active Brownian particles (ABPs; $\alpha = 0$, $D_r = 1$) in one dimension on lattice or two dimensions in continuous space. Black triangles correspond to Supplemental Material movies showing nucleation or spinodal decomposition [46]. For all plots, $v(\rho) = v_0 + \frac{v_1 - v_0}{2}[1 + \tanh(\frac{\rho - \rho_m}{L_f})]$, $K(r) = \exp(-\frac{1}{1-r^2})/Z$ with Z a normalization constant, $\rho_m = 200$, $v_1 = 5$, $L_f = 100$. (b) Common tangent construction on $\phi(R)$ for $v_0 = 20$.

can follow the path of [14,33,34], taking a mean-field approximation of their *fluctuating* hydrodynamics. We first assume a smooth density field so that the velocity can be expanded as [46]

$$v(\tilde{\rho}_i) \approx v(\rho) + \ell^2 v'(\rho)\Delta\rho + \mathcal{O}(\nabla^3), \tag{10}$$

where ρ is evaluated at $\mathbf{r}_i$ and $\ell^2 = \frac{1}{2}\int r^2 K(\mathbf{r})d\mathbf{r}$. Following [33,34], the fluctuating hydrodynamics of QSAPs is then given by $\dot{\rho} = \nabla \cdot (M\nabla g + \sqrt{2M\rho}\Lambda)$ [46], with Λ a unit white noise vector and

$$g_0(\rho) = \log(\rho v); \quad M = \rho\frac{\tau v(\tilde{\rho})^2}{d};$$
$$\kappa(\rho) = -\ell^2\frac{v'}{v}; \quad \lambda(\rho) = 0, \tag{11}$$

where d is the number of spatial dimensions. Here, $\tau \equiv [(d-1)D_r + \alpha]^{-1}$ is the orientational persistence time. The mean-field hydrodynamic equation of QSAPs is then Eq. (1) with the coefficients in Eq. (11). This hydrodynamic description is expected to hold whenever the correlation length is sufficiently small for the mean-field approximation to be valid and the interfaces are sufficiently smooth so that the gradient expansion is justified.

To construct the phase diagram, for a given choice of $v(\rho)$, we first solve Eq. (4) for $R(\rho)$ and use it to obtain both $\phi(R)$ and $h_0(R)$. The binodals then follow via a common-tangent construction on $\phi(R)$ or, equivalently, by setting equal values of h_0 and g_0 in coexisting phases. Note that since $2\lambda + \kappa' \neq 0$ one has $R \neq \rho$.

Figure 1 shows the phase diagrams predicted by our generalized thermodynamics and by QSAP simulations. As expected, the hydrodynamic description works best fairly close to the critical point (but outside a numerically unresolved Ginzburg interval where fluctuations cannot be neglected). This is where interfaces are smoothest and the gradient expansion Eq. (10) most accurate. To determine precisely the binodals, we choose a $v(\rho)$ (given in the caption of Fig. 1) such that MIPS occurs only at large densities, leading to well-separated coexisting densities. Under these conditions, our mean-field approximation works very well: the agreement between predicted and measured binodals is excellent. In contrast, a common tangent construction on $f(\rho)$ defined by $f'(\rho) = g_0(\rho)$ as proposed before [14,33] gives a poorer estimate since it correctly captures the equality of g_0 in both phases but not that of h_0. This reminds us that *gradient terms directly influence the coexisting densities* through Eq. (4)—quite unlike the equilibrium case. As an aside, it is remarkable that for QSAPs we can quantitatively predict the phase diagram of a microscopic model without any fitting parameter; something rare even for equilibrium models.

Beyond the quantitative prediction of the phase diagram, our approach provides insight into the universality of the MIPS seen for QSAPs. For instance, the phase diagram does not depend on the kernel K, which enters Eq. (11) only through the constant ℓ^2 which then cancels from Eq. (4) defining the nonlinear transform $R(\rho)$. Likewise, Fig. 1 includes lattice simulations of QSAPs in 1D where full phase separation is replaced by alternating domains (whose densities obey the predicted binodal values), and confirms the equivalence of continuous (ABP) and discrete (RTP) angular relaxation dynamics for QSAPs [33,34].

PFAPs. We now consider self-propelled particles, of diameter σ, in 2D, interacting via a short-range repulsive pair potential V (see [46] for details):

$$\dot{\mathbf{r}}_i = -\sum_j \nabla_i V(|\mathbf{r}_i - \mathbf{r}_j|) + \sqrt{2D_t}\boldsymbol{\xi}_i + v_0\mathbf{u}_i;$$
$$\dot{\theta}_i = \sqrt{2D_r}\eta_i.$$

Here a microscopic mobility multiplying the first term was set to unity; $\mathbf{u}_i = (\cos\theta_i, \sin\theta_i)$, and $\eta_i, \boldsymbol{\xi}_i$ are unit Gaussian white noises. For simplicity, we only include continuous rotational diffusion, but we expect our results to stand for tumbles as well since this difference has been shown to have a negligible effect on the phase equilibria [34]. MIPS occurs in this system if the Péclet number $\mathrm{Pe} = 3v_0/(\sigma D_r)$ exceeds a threshold value $\mathrm{Pe}_c \sim 60$ [16–19].

We follow [29,47] to derive a fluctuating hydrodynamics for the stochastic density $\hat{\rho}(\mathbf{r}) = \sum_{i=1}^N \delta(\mathbf{r} - \mathbf{r}_i)$, the deterministic limit of which gives a coarse-grained equation for the mean density field. On time scales larger than D_r^{-1}, in our phase-separated setup with a flat interface parallel to $\hat{\mathbf{y}}$, the dynamics is given by $\dot{\rho} = \partial_x^2 g$ [29], with

$$g([\rho],x) = D_t\rho + \frac{v_0^2}{2D_r}(\rho + m_2) + \hat{I}_2 - \frac{v_0 D_t}{D_r}\partial_x m_1 + P_D;$$
$$P_D = \int_{-\infty}^{x} dx \int \partial_x V(\mathbf{r}' - \mathbf{r})\langle\hat{\rho}(\mathbf{r}')\hat{\rho}(\mathbf{r})\rangle d^2\mathbf{r}';$$
$$\hat{I}_2 = -\frac{v_0}{D_r}\int \partial_x V(\mathbf{r}' - \mathbf{r})\langle\hat{\rho}(\mathbf{r}')\hat{m}_1(\mathbf{r})\rangle d^2\mathbf{r}'. \tag{12}$$

Here, $\hat{m}_n = \sum_{i=1}^N \delta(\mathbf{r} - \mathbf{r}_i)\cos(n\theta_i)$ and $m_n = \langle\hat{m}_n\rangle$, where $\langle\cdots\rangle$ represent averages over noise realizations. The lack of steady-state current shows g to be uniform in the phase-separated system, equal to some constant $\bar{g}$.

For homogeneous systems the expression for g in Eq. (12) reduces exactly to the equation of state (EOS) found previously for the mechanical pressure P of PFAPs [29]. Thus g is equal

between phases, as it was for QSAPs, but now it represents pressure, not chemical potential. Moreover, Eq. (12) generalizes the pressure EOS of [29] to inhomogeneous situations. It can formally be written $g = g_0(\rho(x)) + g_{\rm int}([\rho],x)$ where $g_0(\rho)$ is the pressure in a notionally homogeneous system with average density ρ, and the "interfacial" term $g_{\rm int}$ represents all nonlocal corrections to this. The form of g used in Eq. (1) can then be viewed as a gradient expansion of Eq. (12) for PFAPs.

One way forward would be to make that expansion (or perhaps avoid it by using a closed-form ansatz for $g_{\rm int}$), and then find $R(\rho)$ and $\phi(R)$ analytically as was done for QSAPs above. Here, however, we proceed differently, approximating instead the local part, $g_0(\rho)$, of g in Eq. (12) by a well benchmarked, semiempirical EOS, with parameters constrained by simulations of uniform phases at $\mathrm{Pe} = 40 < \mathrm{Pe}_c$ [46]. We thus retain the *exact structure* of the nonlocal terms, $g_{\rm int}(x) \equiv g([\rho],x) - g_0(\rho(x))$ in Eq. (12), but find them numerically. Although less predictive than knowing such terms algebraically, our method clearly illustrates how they select the binodals. Furthermore, $g_{\rm int}$ includes all orders in gradient and hence does not rely on a gradient expansion, contrary to Eq. (1).

We then proceed as in Eq. (3) but, instead of R, now using the volume per particle $v \equiv \rho^{-1}$. The integral $\int_{x_g}^{x_\ell}(g - g_0)\,\partial_x v\,dx$ then admits two equivalent expressions

$$\int_{v_\ell}^{v_g} [g_0(v) - \bar{g}]dv = \int_{x_g}^{x_\ell} g_{\rm int}\,\partial_x v\,dx. \tag{13}$$

Here $g_0(v)$ is the pressure-volume EOS, so that the nonzero value of the right-hand integral *directly* quantifies violation of the Maxwell construction. A fully predictive theory would evaluate the right-hand side integral and then solve $g_0(v_\ell) = g_0(v_g) = \bar{g}$ together with Eq. (13) to obtain the values of the binodals v_ℓ and v_g. In practice, we measure $g(x)$ numerically via Eq. (12) from which we subtract $g_0(\rho(x))$ and integrate over space to obtain the numerical value of the right-hand side of Eq. (13). Crucially, $\bar{g}$, v_g, and v_ℓ are not inputs here, but are found by solving Eq. (13). Concretely this is done via a modified Maxwell construction: The binodals correspond to the intersect between the function $g_0(v)$ and a horizontal line of (unknown) ordinate $\bar{g}$ since $g_0(v_\ell) = g_0(v_g) = \bar{g}$. We then adjust the value of $\bar{g}$ to solve Eq. (13). This construction is illustrated in Fig. 2, and is accurately obeyed by simulations, unlike the equilibrium Maxwell construction, which (notwithstanding [37]) clearly fails to account for the phase equilibria of PFAPs where interfacial terms again directly enter.

In this Rapid Commuication, we have shown how to build a generalized theory of phase-separating scalar active matter starting from a generalized Cahn-Hilliard description derived on symmetry grounds. Our work accounts for the phase equilibria of two important classes of self-propelled particles, PFAPs and QSAPs, which each undergo MIPS. In contrast to equilibrium systems, interfacial contributions to pressure and/or chemical potential generically affect the binodal densities at coexistence [23,29]. We have given in Eqs. (2) and (6) an *explicit construction* for the binodals at leading nontrivial order in a gradient expansion. This is quantitatively accurate for MIPS in QSAPs at high density. In Eq. (13) we have given a more general construction that holds

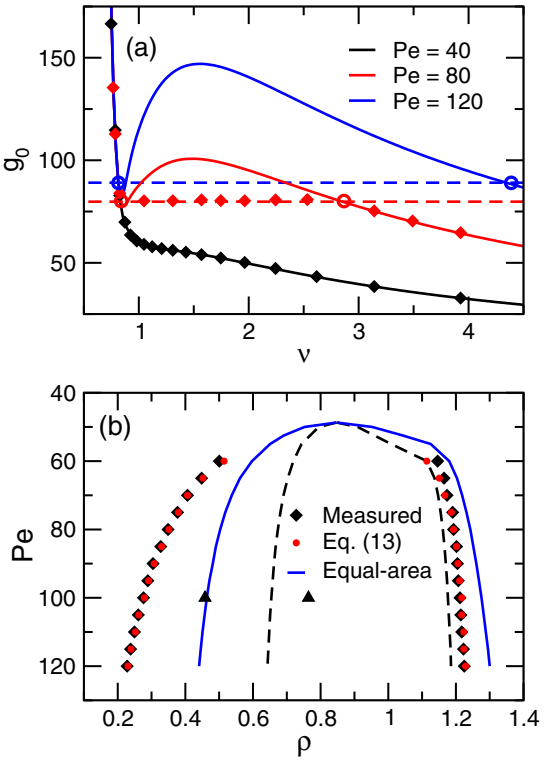

FIG. 2. (a) Mechanical pressure of PFAPs. Semiempirical EOS $g_0(v)$ (line) vs numerical measurements (symbols) for various Pe. Open symbols correspond to binodals and horizontal lines to the pressure $\bar{g}$ predicted by Eq. (13). (b) Corresponding phase diagrams obtained via the modified (red; see text) and the equal-area (blue) Maxwell constructions, compared with numerically measured binodals (black). Dashed lines correspond to the spinodals $g_0'(\rho) = 0$. Black triangles correspond to Supplemental Material movies showing nucleation or spinodal decomposition [46].

beyond the gradient expansion; we tested it using numerical data on PFAPs. In practice, our results are obtained by deriving the coexisting densities of fully phase-separated profiles in the steady state. Extending our formalism to account for the dynamical convergence to this state is an exciting challenge left for future works. Similarly, the fate of our generalized thermodynamic formalism when more than one conserved field is present is an open question.

Interestingly, QSAPs and PFAPs share the same mathematical structure but their coexisting densities are selected by equating intensive observables which have different physical interpretations. In particular, the mechanical pressure is identical in coexisting phases for PFAPs, but not for QSAPs, due to the lack of an effective momentum conservation in the latter case [38]. This fundamental difference is well captured by our formalism which indeed leads to different observables g for the two models.

Beyond understanding the phase equilibria of active matter, we hope that our approach will pave the way toward a more general definition of intensive thermodynamic parameters [48–50] for active systems. Building a thermodynamic theory of active matter would further improve our understanding and control of these intriguing systems and has become a central question in the field [3,14,23–25,29,34,36,37,39,51–56].

Acknowledgments. We thank M. Kardar and H. Touchette for discussions. A.P.S. acknowledges funding through a PLS fellowship from the Gordon and Betty Moore Foundation. J.S. is funded by a Project Grant from the Swedish Research Council (Grant No. 2015-05449). M.E.C. is funded by the Royal Society. This work was funded in part by EPSRC Grant No. EP/J007404. Y.K. is supported by an I-CORE Program of the Planning and Budgeting Committee of the Israel Science Foundation and an Israel Science Foundation grant. J.T. is funded by ANR grant Bactterns. J.T. and Y.K. acknowledge a joint CNRS-MOST travel grant. The PFAP simulations were performed on resources provided by the Swedish National Infrastructure for Computing (SNIC) at LUNARC.

A.P.S. and J.S. contributed equally to this work.

[1] W. F. Paxton, K. C. Kistler, C. C. Olmeda, A. Sen, S. K. St. Angelo, Y. Cao, T. E. Mallouk, P. E. Lammert, and V. H. Crespi, J. Am. Chem. Soc. **126**, 13424 (2004).
[2] J. Deseigne, O. Dauchot, and H. Chaté, Phys. Rev. Lett. **105**, 098001 (2010).
[3] J. Palacci, C. Cottin-Bizonne, C. Ybert, and L. Bocquet, Phys. Rev. Lett. **105**, 088304 (2010).
[4] S. Thutupalli, R. Seemann, and S. Herminghaus, New J. Phys. **13**, 073021 (2011).
[5] I. Buttinoni, J. Bialké, F. Kümmel, H. Löwen, C. Bechinger, and T. Speck, Phys. Rev. Lett. **110**, 238301 (2013).
[6] M. Ballerini, N. Cabibbo, R. Candelier, A. Cavagna, E. Cisbani, I. Giardina, V. Lecomte, A. Orlandi, G. Parisi, A. Procaccini *et al.*, Proc. Natl. Acad. Sci. USA **105**, 1232 (2008).
[7] V. Schaller, C. Weber, C. Semmrich, E. Frey, and A. R. Bausch, Nature (London) **467**, 73 (2010).
[8] Y. Sumino, K. H. Nagai, Y. Shitaka, D. Tanaka, K. Yoshikawa, H. Chaté, and K. Oiwa, Nature (London) **483**, 448 (2012).
[9] H. H. Wensink, J. Dunkel, S. Heidenreich, K. Drescher, R. E. Goldstein, H. Löwen, and J. M. Yeomans, Proc. Natl. Acad. Sci. USA **109**, 14308 (2012).
[10] M. Marchetti, J. Joanny, S. Ramaswamy, T. Liverpool, J. Prost, M. Rao, and R. A. Simha, Rev. Mod. Phys. **85**, 1143 (2013).
[11] A. Bricard, J.-B. Caussin, N. Desreumaux, O. Dauchot, and D. Bartolo, Nature (London) **503**, 95 (2013).
[12] J. Stenhammar, R. Wittkowski, D. Marenduzzo, and M. E. Cates, Sci. Adv. **2**, e1501850 (2016).
[13] M. E. Cates and J. Tailleur, Annu. Rev. Condens. Matter Phys. **6**, 219 (2015).
[14] J. Tailleur and M. Cates, Phys. Rev. Lett. **100**, 218103 (2008).
[15] A. Thompson, J. Tailleur, M. Cates, and R. Blythe, J. Stat. Mech. (2011) P02029.
[16] Y. Fily and M. C. Marchetti, Phys. Rev. Lett. **108**, 235702 (2012).
[17] G. S. Redner, M. F. Hagan, and A. Baskaran, Phys. Rev. Lett. **110**, 055701 (2013).
[18] J. Bialké, H. Löwen, and T. Speck, Europhys. Lett. **103**, 30008 (2013).
[19] J. Stenhammar, A. Tiribocchi, R. J. Allen, D. Marenduzzo, and M. E. Cates, Phys. Rev. Lett. **111**, 145702 (2013).
[20] A. Wysocki, R. G. Winkler, and G. Gompper, Europhys. Lett. **105**, 48004 (2014).
[21] I. Theurkauff, C. Cottin-Bizonne, J. Palacci, C. Ybert, and L. Bocquet, Phys. Rev. Lett. **108**, 268303 (2012).
[22] R. Soto and R. Golestanian, Phys. Rev. E **89**, 012706 (2014).
[23] R. Wittkowski, A. Tiribocchi, J. Stenhammar, R. J. Allen, D. Marenduzzo, and M. E. Cates, Nat. Commun. **5** (2014).
[24] S. C. Takatori, W. Yan, and J. F. Brady, Phys. Rev. Lett. **113**, 028103 (2014).
[25] T. Speck, J. Bialké, A. M. Menzel, and H. Löwen, Phys. Rev. Lett. **112**, 218304 (2014).
[26] R. Matas-Navarro, R. Golestanian, T. B. Liverpool, and S. M. Fielding, Phys. Rev. E **90**, 032304 (2014).
[27] A. Zöttl and H. Stark, Phys. Rev. Lett. **112**, 118101 (2014).
[28] A. Suma, G. Gonnella, D. Marenduzzo, and E. Orlandini, Europhys. Lett. **108**, 56004 (2014).
[29] A. P. Solon, J. Stenhammar, R. Wittkowski, M. Kardar, Y. Kafri, M. E. Cates, and J. Tailleur, Phys. Rev. Lett. **114**, 198301 (2015).
[30] G. S. Redner, C. G. Wagner, A. Baskaran, and M. F. Hagan, Phys. Rev. Lett. **117**, 148002 (2016).
[31] M. J. Schnitzer, Phys. Rev. E **48**, 2553 (1993).
[32] C. Liu, X. Fu, L. Liu, X. Ren, C. K. Chau, S. Li, L. Xiang, H. Zeng, G. Chen, L.-H. Tang *et al.*, Science **334**, 238 (2011).
[33] M. Cates and J. Tailleur, Europhys. Lett. **101**, 20010 (2013).
[34] A. Solon, M. Cates, and J. Tailleur, Eur. Phys. J.: Spec. Top. **224**, 1231 (2015).
[35] P. C. Hohenberg and B. I. Halperin, Rev. Mod. Phys. **49**, 435 (1977).
[36] A. P. Solon, Y. Fily, A. Baskaran, M. E. Cates, Y. Kafri, M. Kardar, and J. Tailleur, Nat. Phys. **11**, 673 (2015).
[37] S. C. Takatori and J. F. Brady, Phys. Rev. E **91**, 032117 (2015).
[38] Y. Fily, Y. Kafri, A. P. Solon, J. Tailleur, and A. Turner, J. Phys. A: Math. Theor. **51**, 044003 (2018).
[39] X. Yang, M. L. Manning, and M. C. Marchetti, Soft Matter **10**, 6477 (2014).
[40] Note that a generic third-order expansion $\mathbf{J} = \alpha\nabla\rho - \kappa\nabla\Delta\rho + \lambda\nabla(\nabla\rho)^2 + [\beta(\nabla\rho)^2 + \gamma\Delta\rho]\nabla\rho$ is formally equivalent to (1), at this order, using for instance $M = 1 + (\frac{\beta}{\alpha} - \frac{\lambda'}{\alpha})(\nabla\rho)^2 + (\frac{\gamma}{\alpha} + \frac{\kappa'}{\alpha})\Delta\rho$ and g_0 such that $g_0'(\rho) = \alpha(\rho)$. Here, however, we restrict ourselves to Eq. (1) with a positive definite M.
[41] A. J. Bray, Adv. Phys. **51**, 481 (2002).
[42] Note that we define g so that M is positive.
[43] S. M. Fielding and P. D. Olmsted, Eur. Phys. J. E **11**, 65 (2003).
[44] J. W. Cahn and J. E. Hilliard, J. Chem. Phys. **28**, 258 (1958).
[45] C. Kipnis and C. Landim, *Scaling Limits of Interacting Particle Systems* (Springer Science & Business Media, Berlin, 2013), Vol. 320.
[46] See Supplemental Material at http://link.aps.org/supplemental/10.1103/PhysRevE.97.020602, which includes Refs. [57–59], for details on the simulations and two movies.
[47] F. Farrell, M. Marchetti, D. Marenduzzo, and J. Tailleur, Phys. Rev. Lett. **108**, 248101 (2012).
[48] E. Bertin, O. Dauchot, and M. Droz, Phys. Rev. Lett. **96**, 120601 (2006).
[49] E. Bertin, K. Martens, O. Dauchot, and M. Droz, Phys. Rev. E **75**, 031120 (2007).

[50] R. Dickman, New J. Phys. **18**, 043034 (2016).
[51] F. Ginot, I. Theurkauff, D. Levis, C. Ybert, L. Bocquet, L. Berthier, and C. Cottin-Bizonne, Phys. Rev. X **5**, 011004 (2015).
[52] J. Bialké, J. T. Siebert, H. Löwen, and T. Speck, Phys. Rev. Lett. **115**, 098301 (2015).
[53] T. F. Farage, P. Krinninger, and J. M. Brader, Phys. Rev. E **91**, 042310 (2015).
[54] U. M. B. Marconi and C. Maggi, Soft Matter **11**, 8768 (2015).
[55] E. Fodor, C. Nardini, M. E. Cates, J. Tailleur, P. Visco, and F. van Wijland, Phys. Rev. Lett. **117**, 038103 (2016).
[56] S. Paliwal, J. Rodenburg, R. van Roij, and M. Dijkstra, New J. Phys. **20**, 015003 (2018).
[57] S. Plimpton, J. Comput. Phys. **117**, 1 (1995).
[58] M. P. Allen and D. J. Tildesley, *Computer Simulation of Liquids* (Oxford University Press, New York, 1989).
[59] D. S. Dean, J. Phys. A: Math. Gen. **29**, L613 (1996).